Transition Metal Mediated Epoxidation as Test Case for the Performance of Different Density Functionals: A Computational Study

Luigi Cavallo and Heiko Jacobsen*,†

Department of Chemistry, Università di Salerno, Via Salvador Allende, Baronissi (SA) I-84081, Italy

Received: January 23, 2003; In Final Form: May 13, 2003

Energy profiles for olefin epoxidation with the cationic $[Mn(acacen')]^+$ catalyst (acacen′ = $^-O(CH)_3N-C_2H_4-N(CH)_3O^-$) have been calculated using pure (BP86) and hybrid (B3LYP) density functional methodologies. For the reaction, triplet and quintet energy hyper surfaces have been considered. The BP86 calculations allow for a rationalization of a reaction occurring under spin conservation. On the other hand, the B3LYP calculations suggest a reaction profile involving an early spin-crossing step, strongly supporting two-state reactivity. Further, the BP86 calculations suggest the existence of a metallacycle as possible reaction intermediate, a proposition not supported by the B3LYP approach. The two different computational approaches result not only in a *quantitatively*, but also in a *qualitatively* different description of the epoxidation reaction. This in turn implies different models for chirality transfer associated with related reactions employing chiral catalytic systems.

Introduction

With the event of density functional theory (DFT) in chemistry,[1] major strides have been made in the area of computational transition metal chemistry,[2,3] which opened up new avenues for chemical research, such as the field of computational organometallic chemistry.[4] Over the last 10 years, DFT has developed into a well-accepted research tool not only for the theoretically,[5,6] but also for the experimentally inclined chemist,[7] being at the verge of adopting the status of a routine method in chemical research. However, although the basic theorems on which DFT is based state the existence of a precise formulation of molecular energies as a functional of the electron density,[8,9] it is well-known that the exact form of that functional is not known.

Ingenuity and intuition play a key role in the development of *approximate* density functional theory, suitable for the treatment of real chemical problems, and *approximate* DFT has repeatedly been characterized as an essentially semiempirical method.[10] If one accepts this judgment, one has to add that approximate DFT introduces a new quality of semiempirical procedures since the level of reasoning and the foundation of the approximations are on a much higher level, compared to common semiempirical methods.

Many research efforts are devoted to improve current density functionals, and to design new density functionals geared toward specific applications.[11] The generalized gradient approximation (GGA), and in particular the combination of the nonlocal gradient corrections for exchange due to Becke,[12] and for correlation due to Perdew,[13] BP86, have been shown to provide a reliable tool for energetics and thermodynamics of transition metal complexes.[2,3]

The so-called hybrid methods, which combine the DFT and Hartree−Fock (HF) approaches in the description of the exchange energy, and which were first proposed by Becke,[14,15] are by now considered to be the method of choice in many areas of DFT calculations. In particular, the B3LYP functional,[16] introduced in the context of the calculation of vibrational circular dichroism spectra,[17] is often considered the standard approach for many problems in transition metal chemistry.

There exists a vast body of literature comparing the performance of and elucidating the differences between various density functionals; however, comparative studies based on problems from the field of transition metal chemistry are scarce, and began to appear only recently.[4,18−20] In the present work, we will investigate such a problem, choosing a rather pragmatic approach often encountered in computational inorganic chemistry. We hope that this contribution will provide helpful hints for the researcher actively pursuing studies in this field.

Background and Objective

The present work is based on the asymmetric epoxidation of olefins, mediated by chiral Mn-salen catalysts, which was introduced by Katsuki[21] and Jacobsen.[22] This reaction is recognized as one of the most practical methods in the epoxidation of alkenes, and Jacobsen's catalyst **1** is effective for virtually every class of conjugated olefins.

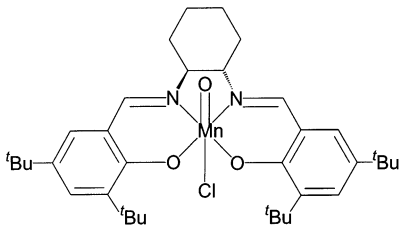

1

We refer the reader to the literature for reviews dealing with the scope and potential of the Jacobsen-Katsuki reaction.[23−29]

The mechanism of the Jacobsen-Katsuki reaction is highly debated,[30] and a controversy has erupted in the literature regarding the presence of a radical[31] or a metallacycle[32] as intermediate species during the course of the epoxidation

† Current address: KemKom, 1864 Burfield Avenue, Ottawa, Ontario, K1J 6T1, Canada. E-mail: jacobsen@kemkom.com.

10.1021/jp034194r CCC: $25.00
Published on Web 06/13/2003

reaction. Several experimental studies dealing with different mechanistic aspects have since then been devoted to this problem.[33−36]

Given the importance of the Jacobsen-Katsuki reaction, it is not surprising that various DFT calculations dealing with this topic have appeared in the literature.[37−46] One of the challenges here lies in the correct electronic description of the catalytically active species, since several spin states, including singlet, triplet, and quintet states, are conceivable for the transition metal complexes involved. Most of the studies employ a simplified model system for the Mn-salen catalyst, as for example the cationic or neutral model compounds $[Mn(acacen')]^+$ and ClMn(acacen′), respectively (acacen′ = $^-O(CH)_3N-C_2H_4-N(CH)_3O^-$), and a simplified model olefin, often ethylene. The DFT functionals used in these studies include the pure BP86 as well as the hybrid B3LYP functional.

The first two computational studies, addressing the mechanism of olefin epoxidation, resulted in strikingly different scenarios for the oxidation step. Using the $[Mn(acacen')]^+$ model catalyst, the B3LYP study of Svensson and co-workers[37] explains the mechanism of the Jacobsen-Katsuki epoxidation in terms of two-state reactivity.[47] It is suggested that the reaction begins on the triplet surface, followed by spin change to the quintet surface. The point at which the spin-crossing occurs then determines the stereochemistry of the reaction. From the results of a BP86 study using the neutral model catalyst ClMn(acacen′), we concluded that the oxidation reaction is likely to occur on the triplet surface.[39] On the basis of this reaction profile, a model could be developed, which ties the enantioselectivity in the epoxidation reaction to the first C−O bond formation step.[44,46] We suggested that the role of the functional group conjugated to the olefinic double bond is to confer regioselectivity to the substrate attack at the oxo ligand of the catalyst, required for high enantiomeric discrimination.[44]

A recent study of Abashkin and co-workers addresses the question of the performance of different density functionals in the context of the Jacobsen-Katsuki epoxidation reaction, putting a main emphasis on quantitative differences.[43] However, Abashkin and co-workers only use a restricted basis set in their calculations, and we recently showed that characteristic properties of the $[Mn(acacen')]^+$ and ClMn(acacen′) systems indeed depended on the choice of basis set.[45] Moreover, the B3LYP calculations performed by Abashkin are single point calculations on the BP86 geometries, and both B3LYP and CCSD(T) calculations were performed only for the simple Mn═O species in the absence of any olefin. Therefore, while the work of Abashkin slightly suggests that BP86 could perform better than B3LYP, a complete and systematic study of the different performances of the BP86 and B3LYP approaches along the whole reaction path is still missing. In fact, up to now this analysis has been performed comparing results obtained with different model systems (cationic or neutral), different basis set (Slater-type orbitals versus Gaussian-type obitals), and the only computationally consistent comparison of Abashkin is limited by the fact that it has been performed on one specific system only, and using the BP86 geometries.

It is thus not obvious whether the differences between given computational studies actually originate from the different density functionals applied, or from other differences in the computational approach. To clarify this situation, and to provide for an unequivocal opportunity to directly compare the performance of different density functionals, we present BP86 as well as B3LYP calculations for one particular scenario of olefin epoxidation with a manganese model catalyst. To check for the effects of the functionals on the geometries, all the structures discussed here were located with both BP86 and B3LYP functionals. It is not the goal of the present study to focus on the mechanistic aspects of the epoxidation reaction, but rather to compare systematically the results of the two popular DFT approaches. In particular, we want to address the question of whether different DFT approaches not only result in *quantitatively*, but also in *qualitatively* different descriptions for a given chemical reaction, similar to our observations for transition metal hydrides.[48]

Computational Details

Spin-unrestricted density functional calculations were carried out using the Gaussian98 program system.[49] B3LYP calculations utilize Becke's three parameter hybrid functional[15] together with the correlation functional of Lee, Yang, and Parr.[50] For BP86 calculations, gradient corrections were taken from the work of Becke,[12] and the local correlation functional of Perdew[51] together with his correlation gradient corrections[13] was used. Mn was described by the TZV basis of Ahlrichs and co-workers,[52] adding one additional *p*-function ($\alpha = 0.12765$). The remaining elements were described by the SVP basis of Ahlrichs and co-workers.[53] Local minima on the energy hypersurface have been characterized by real frequencies only, whereas transition states have been characterized by one imaginary frequency, corresponding to a molecular displacement along the reaction coordinate.

Results and Discussion

As mentioned above, we will base our work on one particular scenario for the epoxidation reaction, involving the cationic model catalyst precursor $[Mn(acacen')]^+$ **2**, and its oxo species $[O{=}Mn(acacen')]^+$ **3**.

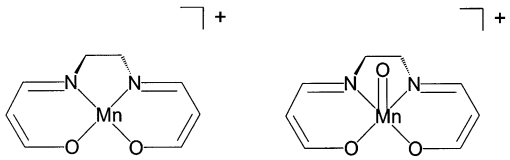

Questions regarding the true nature of the catalytic systems, including the presence as well as the importance of additional axial ligands, and questions regarding alternative reaction mechanisms and catalyst regeneration steps, will not be addressed. Instead, the primary interest lies in the differences of the true density functional and hybrid density functional approaches BP86 and B3LYP. Triplet *T* as well as quintet *Q* energy hypersurfaces will be investigated, and singlet *S* states will only be included for complex **3**. It was suggested that the stepwise reduction of the Mn═O bond,[45] which occurs during the epoxidation reaction, energetically disfavors the singlet state, making it an unlikely candidate for the electronic situation of most of the model complexes investigated in the present scenario.

When talking about spin states and $\langle S^2 \rangle$ values in the framework of density functional theory, a caveat is in order. For an open shell system, with the exception of the highest spin state, it is generally not possible to exactly formulate a given spin state within density functional theory, and $\langle S^2 \rangle$ values are normally constructed for an approximate wave function as Slater determinants from Kohn−Sham orbitals. However, the so-obtained spin-expectation values are routinely reported in

TABLE 1: Relative Energies[a] of Complexes 2 and 3, Optimized for Different Spin States

	2		3		
	T	*Q*	*S*	*T*	*Q*
BP86[b]	62	0	0	27	110
BP86[c]	67	0	0	27	101
B3LYP[b]	112	0	0	11	40
B3LYP[d]	113	0	0	15	47
B3LYP[e]	-	-	6	0	11

[a] In kJ/mol. Literature values have been converted. [b] This work. [c] dζ(p)/tζ(p)-STO basis, ref 45. [d] 6-31G*(HCNOCl)/TZ(Mn) basis, ref 38. [e] DZ basis for ligands, (14s,11p,6d) primitive basis augmented by two p and one diffuse d function contracted to [6s,5p,3d] for Mn, ref 37.

common density functional programs, and are often interpreted and analyzed in applications of density functional theory to molecular problems. Keeping the above-mentioned restriction in mind, we will follow this commonly accepted approach in the present work. The reader is referred to the literature for an analysis of the diagnostic value of $\langle S^2 \rangle$ in Kohn−Sham density functional theory.[54]

The Model Catalysts. In Table 1, compared are the relative energies of optimized geometries for **2** and **3** in different spin states.

The most stable geometry for **2** is a square-planar quintet geometry, followed by the triplet of the same coordination mode. A singulet geometry undergoes a tetrahedral distortion,[38,45] and is not considered any further. An inverted energy ranking is observed for the oxo species, with stability order *S* **3** > *T* **3** > *Q* **3**.

One difference between the BP86 and B3LYP functionals is the fact that the hybrid method energetically favors the *Q* spin states. Thus, in cases where the groundstate is a quintet, such as in **2**, the energy difference between the *Q* and *T* geometries is larger by 50 kJ/mol for the B3LYP calculation, when compared to the BP86 results. On the other hand and for the same reason, *Q* **3** is energetically more disfavored compared to *S* **3** in the BP86 calculation, by 70 kJ/mol.

When comparing with literature values, the BP86 results essentially are in accord with the values obtained from a study employing a Slater-type orbital basis.[45] Also, the B3LYP results compare favorable with the data published by Strassner and Houk,[38] who used the standard 6-31G* Pople basis for the main group elements and a TZ basis for manganese. The different basis sets cause energetic discrepancies between 5 and 10 kJ/mol, but do not affect the general picture.

Significant differences appear when the B3LYP results are compared to the study of Svensson and co-workers.[37] These authors apply for the ligand atoms only a DZ basis without polarization functions. As a result, they observe for the oxo complex **3** three different spin states close in energy, with a different stability ranking *T* **3** > *S* **3** > *Q* **3**. We conclude that the inclusion of polarization functions for atoms belonging to the ligand system is of crucial importance for a proper description of the relative energies of the different spin states.

The Energy Profile of the Epoxidation Reaction. The reaction sequence for the transformation of ethene into oxirane investigated in the present work is illustrated in Scheme 1.

Reference system at zero energy is a weakly coordinated alkene adduct **4**, the alkene approaching the oxo ligand of the catalyst. The transition state for the first C−O bond formation **5** leads to a radical intermediate **6**; the transition state for the second C−O bond formation **7** leads to the epoxy adduct **8**. Further considered is the metallacycle **9**.

In Figure 1, displayed are the BP86 *T* and *Q* energy profiles according to the reaction profile outlined in Scheme 1.

To reach the radical intermediate **6** starting from the reference system **4**, an activation energy of 19 kJ/mol is needed on the *T* energy hypersurface. However, on the *Q* energy hypersurface, the formation of the radical intermediate takes place with virtually no energetic barrier. Resembling the electronic situation of the oxo species **3**, *T* **4** and *Q* **4** are well separated in energy by 77 kJ/mol, suggesting that the initial attack of the olefin takes place on the triplet surface. For the radical intermediate *T* **6**, the quintet state is slightly more stable than the triplet state. However, on the triplet surface there exists a metallacycle *T* **9** at even lower energies, which possibly constitutes the true intermediate in the epoxidation reaction on the triplet surface. The second C−O bond formation occurs without any significant energetic barrier, and leads to the final product **8**, a weak epoxy adduct of the catalyst precursor **2**. The energetic situation of the final product therefore resembles that of **2**, with the quintet

SCHEME 1

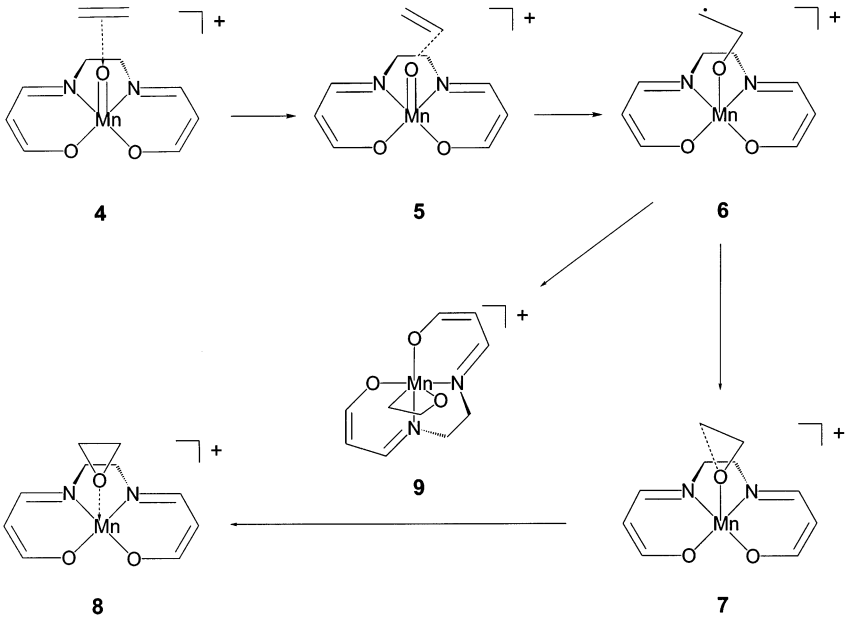

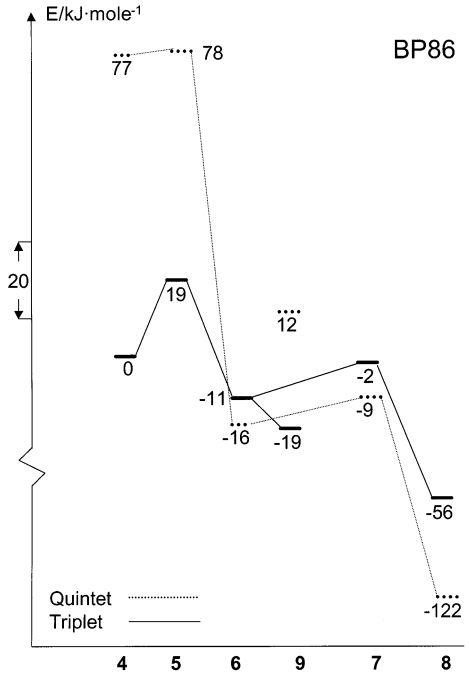

Figure 1. Energy profile on the triplet and quintet surfaces according to BP86 calculations.

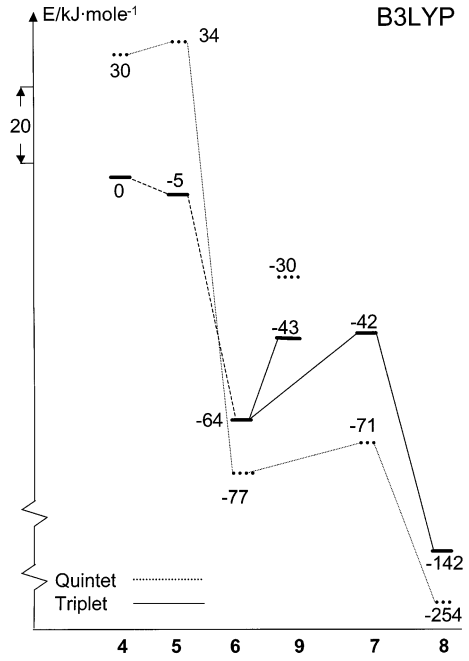

Figure 2. Energy profile on the triplet and quintet surfaces according to B3LYP calculations.

state being energetically favored by 66 kJ/mol. The species *T* **6**, *T* **7**, *T* **9**, *Q* **6**, and *Q* **7** are all close in energy, spanning a range of only 17 kJ/mol. We also note that on the quintet surface the metallacycle *Q* **9** is significantly higher in energy. The BP86 reaction profile obtained in the present work is in accord with earlier studies.[45]

We now turn to the energy profiles obtained from B3LYP calculations, as shown in Figure 2.

In contrast to the BP86 profile, the reference systems *T* **4** and *Q* **4** are separated in energy by only 30 kJ/mol, in favor for the triplet state. While the BP86 *T* **4** structure has an $\langle S^2 \rangle$ value of 2.1, indicating the existence of a pure triplet state, the $\langle S^2 \rangle$ value for B3LYP *T* **4** amounts to 2.6, indicating a situation of mixed spin states. Considering the $\langle S^2 \rangle$ value of 2.1 for the oxo complex B3LYP *T* **3**, it appears that the approaching olefin induces the mixing of triplet and quintet states. On the B3LYP triplet surface, a *T* **5** structure could be optimized, displaying one negative frequency corresponding to a stretching mode of the evolving C−O bond. However, this structure is 5 kJ/mol more stable than reference system *T* **4**, and therefore does not qualify as a true transition state for olefin epoxidation on the B3LYP triplet surface. In contrast, the B3LYP calculations of Svensson and co-workers[37] indicate a first transition state on the triplet surface, which is of similar geometry as the *T* **5** species (vide supra), but which is at higher energy than the reference state. An $\langle S^2 \rangle$ value of 2.8 for *T* **5** indicates a significant amount of spin contamination, suggesting a considerable amount of mixing of the triplet and the quintet states. We interpret the optimized *T* **5** structure as a sign for a possible occurrence of spin crossing during the formation of the first C−O bond. On the *Q* energy hypersurface, the first C−O bond formation occurs without any significant energetic barrier, requiring an energetic activation of 7 kJ/mol. For the radical intermediate, the quintet species *Q* **6** is clearly favored over the triplet *T* **6** by 13 kJ/mol. Again, the *T* **6** structure represents a mixed triplet-quintet state with an $\langle S^2 \rangle$ value of 3.1. On the quintet surface, the second C−O bond formation takes place without any significant energetic barrier, leading to the epoxy adduct *Q* **8**. A metallacycle *Q* **9** is energetically disfavored. On the other hand, on the triplet surface an energetic activation of 22 kJ/mol is required to reach the second transition state, and even the metallacycle *T* **9** is 21 kJ/mol higher in energy than the radical intermediate *T* **6**, contrary to the BP86 case.

Following qualitative description emerges from the results described above: According to the BP86 calculation, the reaction path for epoxidation on the triplet surface is energetically favored over, or can compete with, the energy profile on the quintet surface. No stringent observation is made that suggests a spin crossing to occur. The reaction profile both supports spin conservation as well as spin change processes. If a spin change should occur, it is likely to take place in connection with the second C−O bond formation, or after the final product has formed. The activation energies for the first as well as for the second C−O bond formation are comparable for the *T* and for the *Q* profile. Also, a metallacycle constitutes a viable reaction intermediate on the triplet surface. The B3LYP calculations on the other hand lead to a different description of the epoxidation reaction. In this case, the first C−O bond formation takes place without any significant activation energy. After a radical intermediate is formed, the quintet profile is clearly favored over the triplet profile. For example, the final step in product formation requires a small activation energy of 6 kJ/mol on the quintet surface, but a 16 kJ/mol larger activation energy on the triplet surface. Assuming that the epoxidation is initiated on the triplet surface, the B3LYP calculation suggests a spin crossing to occur before formation of the second C−O bond, and possibly during the process of formation of the first C−O bond. The B3LYP calculations clearly disfavor the occurrence of metallacycles as intermediate species. The picture emerging from the present B3LYP calculations is similar to that drawn by Svensson and co-workers.[37]

The First Transition State 5. Not only the energetic profiles, but also the molecular geometries exhibit different features when determined with different density approaches. As an exemplary case we will discuss different geometries for the first transition state **5**, which has been considered to constitute a key structure in the transfer of chiral information during the epoxidation

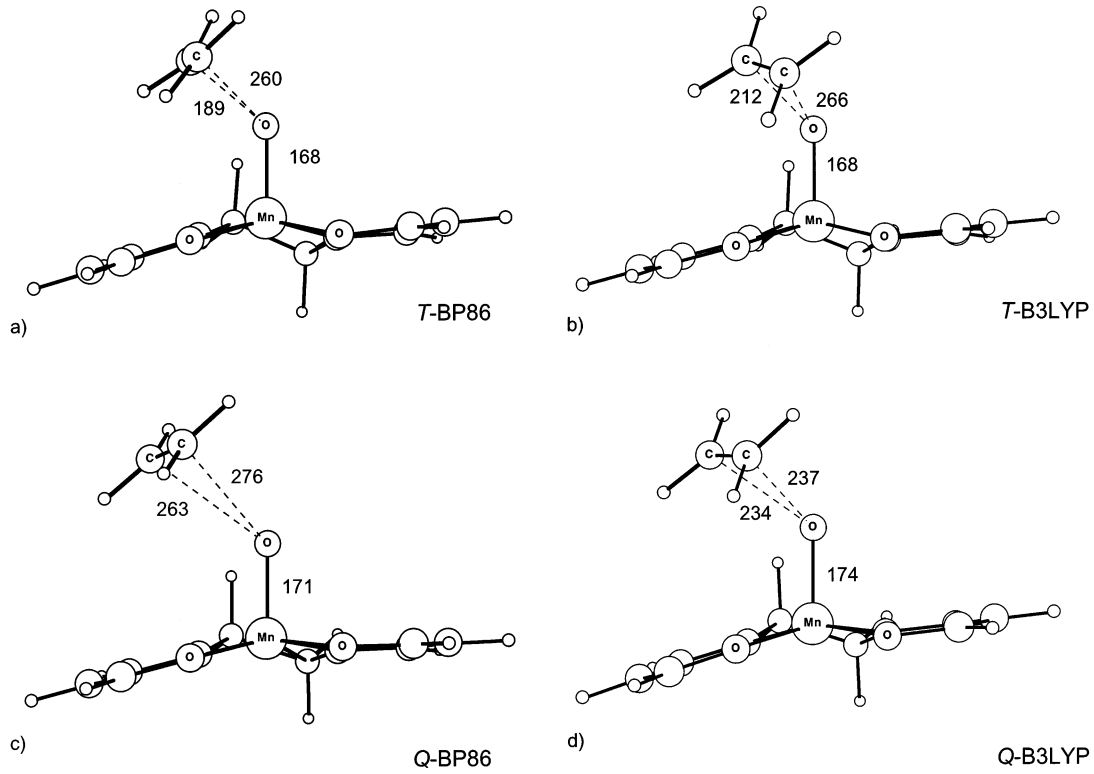

Figure 3. First transition states **5** on different spin surfaces obtained from different density functional calculations: (a) *T*-BP86, (b) *T*-B3LYP, (c) *Q*-BP86, (d) *Q*-B3LYP.

reaction.[33,44] The triplet and quintet geometries according to BP86 and B3LYP calculations are displayed in Figure 3.

On the triplet surface, the BP86 calculation results in an asymmetric first transition state with two different C−O separations of 189 and 260 pm, respectively, indicating the formation of one new C−O bond (Figure 3a). The B3LYP triplet structure (Figure 3b) displays a similar asymmetric approach. However, the separation of the C and O atoms involved in formation of the new bond is significantly larger by 23 pm. As mentioned above, the structure of the first transition state calculated by Svensson and co-workers[37] is similar to B3LYP-*T* **5**, with an asymmetric olefin approach leading to a separation of the C−O bond forming atoms by 212 pm.

On the quintet surface, an early transition state is calculated according to both DFT approaches; however, the C−O separations are about 30 pm shorter in the B3LYP case compared to BP96. Also, the B3LYP *Q* **5** structure (Figure 3d) strongly resembles a synchronous attack of both olefinic C-atoms at the oxo center, whereas for the BP86 *Q* **5** geometry (Figure 3c) two distinct different C−O separations are found.

Energetics of Complex Formations. We close our discussion with a brief analysis of three complex formation reactions, addressing olefin precoordination, reactions 1 and 2, and product liberation, reaction 3.

$$\mathbf{3} + C_2H_4 \rightarrow \mathbf{4} \quad (1)$$

$$\mathbf{3} + C_2H_4 \rightarrow \mathbf{10} \quad (2)$$

$$\mathbf{2} + C_2H_4O \rightarrow \mathbf{8} \quad (3)$$

The energetics for these reactions are collected into Table 2. The energy values ΔE are corrected by zero point energy contribution to result in reaction enthalpies at zero K, ΔH^{0K}.

For olefin precoordination at the site of the oxo ligand, reaction 1, we find only very weakly bonded adducts. The ΔE and ΔH^{0K} values are of comparable in the quintet cases compared to the triplet cases, and are still much smaller than typical values for ligand bond energies.[55] Similar energetics are found for olefin pre-coordination at the free coordination site of the transition metal center, reaction 2, leading to formation of complex **10**.

TABLE 2: Energy Values[a] for Association Reactions 1, 2, and 3

		BP86		B3LYP	
		T	*Q*	*T*	*Q*
(1)	ΔE	−8	−12	−17	−16
	ΔH^{0K}	−6	−9	−15	−12
(2)	ΔE	−8	−23	−11	−20
	ΔH^{0K}	−5	−18	−9	−15
(3)	ΔE	−84	−98	−88	−98
	ΔH^{0K}	−76	−93	−81	−93

[a] In kJ/mol.

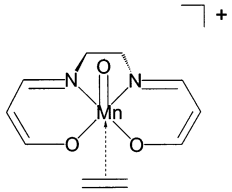

10

For this reaction, precoordination is more favorable on the quintet energy hypersurface, but the calculated bonding energies on any of the spin surfaces considered do not support the notion of a stable olefin complex. Both BP86 and B3LYP calculations agree in the same qualitative finding that, in accord with recent experimental studies,[40] precoordination does not play a major role in epoxidation reactions with cationic Mn catalysts.

For the formation of the epoxide complex **8**, both BP86 and B3LYP calculations result in similar values, indicating that the

quintet complex *Q* **8** is about 10 kJ/mol stronger bonded. Again, contributions due to zero point energy significantly reduces the ΔE estimate, and taken entropic contributions into account,[39] product liberation is not likely to be a critical step in the catalytic cycle of olefin epoxidation.

Conclusion

The present work demonstrates that different density functional approaches might result in qualitatively different chemical interpretations of a given reaction. For the olefin epoxidation with a cationic Mn catalyst, B3LYP calculations suggest a reaction profile involving an early spin-crossing step, whereas the BP86 calculations suggest the possibility of a late spin-crossing step, and also allow for a rationalization of a reaction occurring under spin conservation. Further, the B3LYP calculation excludes the existence of a metallacycle intermediate, whereas the BP86 predicts a metallacycle to be energetically accessible. Both approaches lead to different models for chirality transfer, essential for a basic understanding of the reaction mechanism.[37,44] The possibility for the epoxidation with cationic Mn catalysts to exhibit two-state reactivity is strongly tied to the use of the hybrid density functional method. Our work does not allow judging which computational approach results in a better description of this particular problem. In a view of a recent study involving highly correlated coupled cluster calculations,[43] it seems that for modeling of the Jacobsen-Katsuki reaction the pure BP86 approach is preferably used over the hybrid B3LYP method.

Acknowledgment. Università di Salerno and MURST of Italy generously supported the present work. We thank CIMCF of the University "Federico II" of Napoli for technical assistance, and Professor T. K. Woo at University of Western Ontario and the Sharcnet project for generous access to computer resources.

Supporting Information Available: Listing of Cartesian coordinates and final energies for all optimized geometries, spin expectation values for open-shell systems, as well as imaginary frequencies for transition states.

References and Notes

(1) *Density Functional Methods in Chemistry*; Labanowski, J. K., Anselm, J. W., Eds.; Springer-Verlag: Heidelberg, 1991.
(2) Ziegler, T. *Chem. Rev.* **1991**, *91*, 651.
(3) Ziegler, T. *Can. J. Chem.* **1995**, *73*, 743.
(4) *Computational Organometallic Chemistry*; Cundari, T. R., Ed.; Marcel Dekker: New York, 2001.
(5) *Recent Advances in Density Functional Methods, Parts I & II*; Chong, D. P., Ed.; World Scientific: Singapore, 1997.
(6) *Recent Advances in Density Functional Methods, Part III*; Barone, V., Bencini, A., Fantucci, P., Eds.; World Scientific: Singapore, 2002.
(7) Koch, W.; Holthausen, M. C. *A Chemist's Guide to Density Functional Theory*; Wiley-VCH: Weinheim, 2000.
(8) Hohenberg, P.; Kohn, W. *Phys. Rev. B* **1964**, *136*, 864.
(9) Kohn, W.; Sham, L. J. *Phys. Rev. A* **1965**, *140*, 1133.
(10) Tozer, D. J.; Handy, N. C. *J. Chem. Phys.* **1998**, *108*, 2545.
(11) *Recent Developments and Applications of Modern Density Functional Theory*; Seminario, J. M., Ed.; Elsevier Science: Amsterdam, 1996.
(12) Becke, A. D. *Phys. Rev. A* **1988**, *38*, 3098.
(13) Perdew, J. P. *Phys. Rev. B* **1986**, *33*, 8822.
(14) Becke, A. D. *J. Chem. Phys.* **1993**, *98*, 1372.
(15) Becke, A. D. *J. Chem. Phys.* **1993**, *98*, 5648.
(16) Hertwig, R. H.; Koch, W. *Chem. Phys. Lett.* **1997**, *268*, 345.
(17) Stephens, P. J.; Devlin, F. J.; Chabalowski, C. F.; Frisch, M. J. *J. Phys. Chem.* **1994**, *98*, 11623.
(18) Yanagisawa, S.; Tsuneda, T.; Hirao, K. *J. Chem. Phys.* **2000**, *112*, 545.
(19) Barden, C. J.; Rienstra-Kiracofe, J. C.; Schaefer, H. F. *J. Chem. Phys.* **2000**, *113*, 690.
(20) Yanagisawa, S.; Tsuneda, T.; Hirao, K. *J. Comput. Chem.* **2001**, *22*, 1995.
(21) Irie, R.; Noda, K.; Ito, Y.; Matsumoto, N.; Katsuki, T. *Tetrahedron Lett.* **1990**, *21*, 7345.
(22) Zhang, W.; Loebach, J. L.; Wilson, S. R.; Jacobsen, E. N. *J. Am. Chem. Soc.* **1990**, *112*, 2801.
(23) Jacobsen, E. N. In *Catalytic Asymmetric Synthesis*; Ojima, I., Ed.; VCH: Weinheim, 1993; Chapter 4.2.
(24) Jacobsen, E. N. in *Comprehensive Organometallic Chemistry II*; Wilkinson, G., Stone, F. G. A., Abel, E. W., Hegedus, L. S., Eds.; Pergamon: New York, 1995; Vol. 12, Chapter 11.1.
(25) Katsuki, T. *Coord. Chem. Rev.* **1995**, *140*, 189.
(26) Katsuki, T. *J. Mol. Catal. A* **1996**, *113*, 87.
(27) Dalton, C. T.; Ryan, K. M.; Wall, V. M.; Bousquet, C.; Gilheany, D. G. *Top. Catal.* **1998**, *5*, 75.
(28) Flessner, T.; Doye, S. *J. Prakt. Chem.* **1999**, *341*, 436.
(29) Katsuki, T. *Adv. Synth. Catal.* **2002**, *344*, 131.
(30) Linker, T. *Angew. Chem.* **1997**, *109*, 2150; *Angew. Chem., Int. Ed. Engl.* **1997**, *36*, 2060.
(31) Finney, N. S.; Pospisil, P. J.; Chang, S.; Palucki, M.; Konsler, R. G.; Hansen, K. B.; Jacobsen, E. N. *Angew. Chem.* **1997**, *109*, 1798; *Angew. Chem., Int. Ed. Engl.* **1997**, *36*, 1720.
(32) Linde, C.; Arnold, M.; Norrby, P.-O.; Åckermark, B. *Angew. Chem.* **1997**, *109*, 1802; *Angew. Chem., Int. Ed. Engl.* **1997**, *36*, 1723.
(33) Palucki, M.; Finney, N. S.; Pospisil, P. J.; Güler, M. L.; Ishida, T.; Jacobsen, E. N. *J. Am. Chem. Soc.* **1998**, *120*, 948.
(34) Adam, W.; Stegemann, V. R.; Saha-Möller, C. R. *J. Am. Chem. Soc.* **1999**, *121*, 1879.
(35) Linde, C.; Koliaï, N.; Norrby, P.-O.; Åckermark, B. *Chem. Eur. J.* **2002**, *8*, 2568.
(36) Adam, W.; Roschmann, K. J.; Saha-Möller, C. R.; Seebach, D. *J. Am. Chem. Soc.* **2002**, *124*, 5068.
(37) Linde, C.; Åckermark, B.; Norrby, P.-O.; Svensson, M. *J. Am. Chem. Soc.* **1999**, *121*, 5083.
(38) Strassner, T.; Houk, K. N. *Org. Lett.* **1999**, *1*, 419.
(39) Cavallo, L.; Jacobsen, H. *Angew. Chem.* **2000**, *112*, 602; *Angew. Chem., Int. Ed. Engl.* **2000**, *39*, 589.
(40) Plattner, D. A.; Feichtinger, D.; El-Bahraoui, J.; Wiest, O. *Int. J. Mass Spectrom.* **2000**, *195/196*, 351.
(41) El-Bahraoui, J.; Wiest, O.; Feichtinger, D.; Plattner, D. A. *Angew. Chem.* **2001**, *109*, 1796; *Angew. Chem., Int. Ed. Engl.* **2001**, *40*, 2073.
(42) Feichtinger, D.; Plattner, D. A. *Chem. Eur. J.* **2001**, *7*, 591.
(43) Abashkin, Y. G.; Collins, J. R.; Burt, S. K. *Inorg. Chem.* **2001**, *40*, 4040.
(44) Jacobsen, H.; Cavallo, L. *Chem. Eur. J.* **2001**, *7*, 800.
(45) Cavallo, L.; Jacobsen, H.; *Eur. J. Inorg.* **2003**, 892.
(46) Cavallo, L.; Jacobsen, H. *J. Org. Chem.*, in press.
(47) Schröder, D.; Shaik, S.; Schwarz, H. *Acc. Chem. Res.* **2000**, *33*, 139.
(48) Jacobsen, H. *J. Phys. Chem. A* **2002**, *106*, 6189.
(49) Frisch, M. J.; Trucks, G. W.; Schlegel, H. B.; Scuseria, G. E.; Robb, M. A.; Cheeseman, J. R.; Zakrzewski, V. G.; Montgomery, J. A., Jr.; Stratmann, R. E.; Burant, J. C.; Dapprich, S.; Millam, J. M.; Daniels, A. D.; Kudin, K. N.; Strain, M. C.; Farkas, O.; Tomasi, J.; Barone, V.; Cossi, M.; Cammi, R.; Mennucci, B.; Pomelli, C.; Adamo, C.; Clifford, S.; Ochterski, J.; Petersson, G. A.; Ayala, P. Y.; Cui, Q.; Morokuma, K.; Malick, D. K.; Rabuck, A. D.; Raghavachari, K.; Foresman, J. B.; Cioslowski, J.; Ortiz, J. V.; Stefanov, B. B.; Liu, G.; Liashenko, A.; Piskorz, P.; Komaromi, I.; Gomperts, R.; Martin, R. L.; Fox, D. J.; Keith, T.; Al-Laham, M. A.; Peng, C. Y.; Nanayakkara, A.; Gonzalez, C.; Challacombe, M.; Gill, P. M. W.; Johnson, B.; Chen, W.; Wong, M. W.; Andres, J. L.; Gonzalez, C.; Head-Gordon, M.; Replogle, E. S.; Pople, J. A. *Gaussian 98*, Revision A.5; Gaussian Inc.: Pittsburgh, PA, 1998.
(50) Lee, C.; Yang, W.; Parr, R. G. *Phys. Rev. B* **1988**, *37*, 785.
(51) Perdew, J. P.; Zunger, A. *Phys. Rev. B* **1981**, *23*, 5048.
(52) Schäfer, A.; Huber, C.; Ahlrichs, R. *J. Chem. Phys.* **1994**, *100*, 5829.
(53) Schäfer, A.; Horn, H.; Ahlrichs, R. *J. Chem. Phys.* **1992**, *97*, 2571.
(54) Grafenstein, J.; Cremer, D. *Mol. Phys.* **2001**, *99*, 891.
(55) Marks, T. J. *ACS Sym. Ser*. **1990**, *428*, 1.